Biochimie 150 (2018) 57–69

Contents lists available at ScienceDirect

Biochimie

journal homepage: www.elsevier.com/locate/biochi

Research paper

Phosphorylation-induced conformational changes of photoactivated rhodopsin probed by fluorescent labeling at Cys^{140} and Cys^{316}

Sheerly Rodríguez [a, b, 1], May-Li Silva [c, 2], Gustavo Benaím [c, d], José Bubis [a, *]

[a] Departamento de Biología Celular, Universidad Simón Bolívar, Caracas, Venezuela
[b] Escuela de Química, Facultad de Ciencias, Universidad Central de Venezuela, Caracas, Venezuela
[c] Instituto de Estudios Avanzados IDEA, Caracas, Venezuela
[d] Instituto de Biología Experimental, Facultad de Ciencias, Universidad Central de Venezuela, Caracas, Venezuela

ARTICLE INFO

Article history:
Received 20 January 2018
Accepted 29 April 2018
Available online 4 May 2018

Keywords:
Rhodopsin
Cysteine
Monobromobimane labeling
Fluorescence
Protein conformational changes
Phosphorylation

ABSTRACT

In order to monitor conformational changes following photoactivation and phosphorylation of bovine rhodopsin, the two reactive sulfhydryl groups at Cys^{140} and Cys^{316} were specifically labeled with the monobromobimane (mBBr) fluorophore. Although alterations in conformation after light exposure of rhodopsin were not detected by fluorescence excitation scans (300–450 nm) of the mBBr-labeled protein, the fluorescence signal was reduced ~ 90% in samples containing photoactivated phosphorhodopsin. Predominant labeling at either Cys^{140} or Cys^{316} in light-activated and phosphorylated rhodopsin merely generated a decrease of ~38% and 28%, respectively, in the fluorescence excitation intensity. Thus, neither mBBr-modified Cys^{140} nor mBBr-modified Cys^{316} were involved single-handedly in the remarkable fall seen on the signal following phosphorylation of the protein; rather, the incorporation of phosphate groups on the mBBr-labeled light-activated rhodopsin appeared to affect its fluorescence signal in a cooperative or synergistic manner. These findings demonstrated that the phosphorylation of specific hydroxyl groups at the carboxyl terminal tail of rhodopsin causes definite conformational changes in the three-dimensional fold of the protein. Apparently, amino acid residues that are buried in the interior of the inactive protein become accessible following illumination and phosphorylation of rhodopsin, quenching in turn the fluorescence excitation signal of mBBr-modified rhodopsin.

1. Introduction

In photoreceptor rod cells, light activation of rhodopsin drives the phototransduction cascade that initiates vision [1]. Upon illumination, the inverse agonist 11-*cis*-retinal of rhodopsin is isomerized to its all-*trans* geometry, which represents the chromophore active form. This process leads to the formation of a series of photoproducts that are recognized by their distinctive absorption spectra (photorhodopsin, bathorhodopsin, blue shifted intermediate or BSI, lumirhodopsin, metarhodopsin I, and metarhodopsin II). As a consequence, alterations at the cytoplasmic surface of rhodopsin are produced, and three proteins, the G-protein transducin, rhodopsin kinase, and arrestin-1, are now capable of binding to this region. Eventually, light converts metarhodopsin II that is the activated signaling form of the receptor into metarhodopsin III, which finally dissociates to opsin and free all-*trans*-retinal.

The cysteine thiol groups are widely employed for site-specific protein modification. As indicated in Fig. 1, bovine rhodopsin possesses 10 cysteine residues at positions 110, 140, 167, 185, 187, 222, 264, 316, 322, and 323 [2,3], which have been shown to have the following characteristics: i) Cys^{167}, Cys^{222}, and Cys^{264} are buried within the transmembrane helices; ii) Cys^{110} and Cys^{187} form a

Abbreviations: BCIP, 5-bromo-4-chloro-3-indolyl phosphate; NBT, nitro blue tetrazolium; PMSF, phenylmethylsulfonylfluoride; mBBr, monobromobimane; dmBBr, dibromobimane; qmBBr, monobromotrimethylammoniobimane; ROS, rod outer segments.

* Corresponding author. Laboratorio de Química de Proteínas, Departamento de Biología Celular, División de Ciencias Biológicas, Universidad Simón Bolívar, Apartado 89.000, Valle de Sartenejas, Caracas, 1081-A, Venezuela.
E-mail addresses: sheerly.rodriguez-acosta@danone.com (S. Rodríguez), may-li.silva-prieto@uni-tuebingen.de (M.-L. Silva), gbenaim@idea.gob.ve (G. Benaím), jbubis@usb.ve (J. Bubis).
[1] Present address: Danone, Berlin 50, Longchamps, Buenos Aires, Argentina.
[2] Present address: Systems Neurophysiology, Werner Reichardt Centre for Integrative Neuroscience, University of Tübingen, Otfried-Müller-Str. 25, 72076 Tübingen, Germany.

https://doi.org/10.1016/j.biochi.2018.04.025
0300-9084/

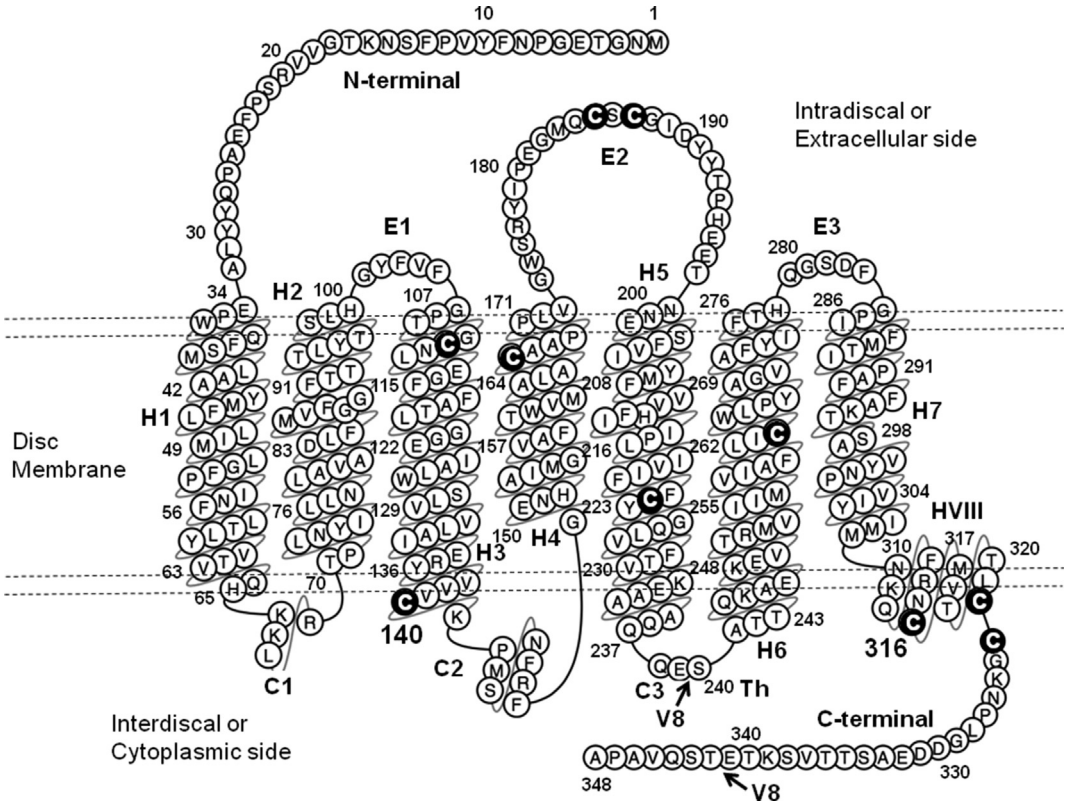

Fig. 1. Two-dimensional model of bovine rhodopsin. Shown is the secondary structure diagram that was acquired from the GPCRdb data base (http://gpcrdb.org/) for *Bos taurus* rhodopsin (PDB ID:1F88; http://gpcrdb.org/construct/1F88/). The polypeptide crosses the disk membrane seven times, and amino acid residues are depicted using the single-letter code abbreviation. The amino-terminal tail (N-terminal) and the intradiscal side or extracellular side (in other G-protein-coupled receptors) is toward the top, and the carboxyl-terminal tail (C-terminal) and cytoplasmic or interdiscal side is toward the bottom. The transmembrane α-helices H1 to H7 and amphipathic helix HVIII are shown. C1, C2, and C3 correspond to the interdiscal or cytoplasmic loops, and E1, E2, and E3 correspond to the intradiscal or extracellular loops. The 10 cysteine residues of the protein at positions 110, 140, 167, 185, 187, 222, 264, 316, 322, and 323 are highlighted in black. Arrows indicate the site of cleavage by the *S. aureus* V8 protease (V8). Dashed lines illustrate an approximate location of the disk membrane.

disulfide bond [4,5] that sterically hinders the modification of the neighboring Cys^{185}; iii) Cys^{322} and Cys^{323} are palmitoylated and attached to the disc membrane [6,7]; and iv) Cys^{140} and Cys^{316} are located at the cytoplasmic side, and are very reactive to sulfhydryl modification reagents [8,9]. Of these two residues, Cys^{316} appears to be more reactive than Cys^{140} [10–13]. Additionally, the C-terminus of rhodopsin has a cluster of serine and threonine residues that are considered hallmarks for multiple phosphorylations [14]. It is known that the light-induced conformational change in rhodopsin exposes these residues at the rhodopsin C-terminal tail, causing their rapid phosphorylation by rhodopsin kinase. Although light-activated rhodopsin can be phosphorylated with up to nine phosphates in vitro [14], liquid chromatography-mass spectrometry or direct sequencing revealed main phosphorylation sites by rhodopsin kinase at Ser^{334}, Ser^{338} and Ser^{343} [15–18]. However, Azevedo et al. [19] have shown that the C-terminal serines and threonines play distinct roles in the desensitization of rhodopsin. It appears that the slower addition of phosphates to the threonines is crucial to promote arrestin-1 binding and completely switch off the protein [19].

Because the intensity and maximal wavelength of fluorescence are sensitive to environmental changes, fluorescent dyes are excellent probes for detecting local conformational changes in proteins. Bromobimanes are highly efficient labeling agents for proteins, giving rise to fluorescently labeled materials that exhibit high quantum yields of fluorescence, and are especially stable [20,21]. The primary sites for labeling in proteins are reactive sulfhydryl groups, and the fluorescent moiety is small since it is only formed by two pentacyclic rings. As such, these compounds provide minimum of opportunity for perturbation of the protein conformation near those sites at which they are covalently bound. Here, we used the two accessible thiol groups of the native Cys^{140} and Cys^{316} of rhodopsin to attach specifically the monobromobimane (mBB) fluorophore and determine the conformational changes induced in rhodopsin following photoactivation and phosphorylation of the receptor protein. Preliminary results of this study were presented in the Colloquium Biochimie: Bioquímica y sus aplicaciones at Universidad de Carabobo, Valencia, Venezuela [22].

2. Materials and methods

2.1. Materials

Bovine eyes were obtained from the nearest abattoir (Beneficiadora Diagon, C.A., Matadero Caracas, Venezuela). Retinas were extracted in the dark, under red light, and were maintained frozen at - 80 °C. Reagents were purchased from the following sources: anti-rabbit IgG alkaline phosphatase conjugate, Pierce; 5-bromo-4-chloro-3-indolyl phosphate (BCIP), nitro blue tetrazolium (NBT), middle range molecular weight protein markers, Promega; *n*-dodecyl β-D-maltoside, *Staphylococcus aureus* V8 protease (*aka* endoproteinase Glu-C), phenylmethylsulfonylfluoride (PMSF), *N*-ethylmaleimide, L-cysteine, Sigma; rabbit polyclonal anti-phosphoserine antibodies, Benchmark prestained molecular weight protein markers, Invitrogen; monobromobimane (mBBr),

dibromobimane (dmBBr), monobromotrimethylammoniobimane (qmBBr), Calbiochem; nitrocellulose membranes (0.45 μm), Advantec.

2.2. Preparation of rod outer segments (ROS) and dark-depleted ROS membranes

ROS were isolated from frozen bovine retinas as described previously [23]. Although rhodopsin is the major protein (>90%) [1], other proteins are also present in purified ROS. As formerly shown, most of these soluble and peripheral proteins can be extracted in the dark using hypotonic buffer, and little protein besides rhodopsin remains with the washed membranes [24,25]. Moreover, since the procedure is carried out in the dark, rhodopsin is maintained completely functional. These hypotonically-washed membranes are known as dark-depleted ROS membranes. Dark-depleted ROS membranes were prepared by washing ROS with 5 mM Tris-HCl (pH 7.4), 2 mM EDTA, and 5 mM β-mercaptoethanol until no peripheral proteins were released. ROS and washed ROS membranes were suspended in 100 mM potassium phosphate (pH 6.8), 5 mM magnesium acetate, and 5 mM β-mercaptoethanol, and stored in the dark at - 80 °C. The concentration of rhodopsin was determined using its molar extinction coefficient (40,700 $M^{-1}cm^{-1}$ at 500 nm) [26].

2.3. Preparation of an enriched-fraction of rhodopsin kinase

A partially purified fraction of rhodopsin kinase was acquired according to Medina et al. [27]. Briefly, freshly isolated ROS were extensively washed in the dark with 100 mM potassium phosphate (pH 6.8), 5 mM magnesium acetate, 5 mM β-mercaptoethanol, and 0.1 mM PMSF. Then, the isotonically washed ROS were hypotonically extracted in the dark with 5 mM Tris-HCl (pH 7.4), 5 mM magnesium acetate, 5 mM β-mercaptoethanol, and 0.1 mM PMSF. An enriched fraction of rhodopsin kinase was obtained in the supernatant following centrifugation. The partially purified rhodopsin kinase fraction also contained other peripheral ROS contaminating proteins such as transducin and arrestin-1.

2.4. Phosphorylation of photoactivated rhodopsin

Samples containing dark-depleted ROS membranes (50 μg of rhodopsin) were incubated with a 50 μl aliquot of an enriched fraction of rhodopsin kinase (10 μg of total protein), in the presence of 50 mM Tris-HCl (pH 8.0), 5 mM magnesium acetate, 20 mM potassium fluoride, and 50 μM ATP. Experiments were initiated in the dark under red light, followed by illumination (white light, 200 Watts) for 30 min, at room temperature. Samples were centrifuged at 100,000 *g*, for 20 min, at 4 °C, and the resulting pellets contained the photoactivated and phosphorylated rhodopsin. Phosphorhodopsin was analyzed by immunoblotting using rabbit polyclonal anti-phosphoserine antibodies (dilution 1:125). Blots were first treated with alkaline phosphatase-conjugated secondary antibodies against rabbit IgG (dilution 1:2000), and then with BCIP and NBT (according to the instructions of the supplier) to visualize the immunoreactive bands.

2.5. Fluorescent labeling of rhodopsin with bimane derivatives

Bimane derivatives (mBBr, dmBBr and qmBBr) were first dissolved in either acetonitrile or dimethyl sulfoxide. Washed ROS membranes containing 2–4 mg of rhodopsin were incubated overnight (16 h), at 4 °C, and under constant agitation, with a 20 fold molar excess of mBBr, dmBBr or qmBBr, in a buffer containing 5 mM Mes, 50 mM Hepes, and 1 mM EDTA (pH 6.7). Experiments were carried out in the dark, under illumination, and following illumination and phosphorylation of rhodopsin. The reaction mixtures were centrifuged at 100,000 *g*, for 20 min, at 4 °C, and the resulting pellets were washed in the same buffer containing a 20 fold molar excess of L-cysteine over rhodopsin. Finally, excess label was removed by repeated washing with 5 mM Mes, 50 mM Hepes, and 1 mM EDTA (pH 6.7), until no free label was detected in the supernatant. Under these conditions, the two reactive sulfhydryl groups of rhodopsin at Cys^{140} and Cys^{316} were modified by the bimane fluorophores. Covalent attachment of the labels was verified by subjecting the rhodopsin samples to SDS-PAGE analysis [28]. After electrophoresis the gel slabs were visualized by UV irradiation using a transilluminator, and photographed under UV illumination (360 nm), either immediately or following a washing step with 25% isopropanol and 10% acetic acid for ~ 24 h.

2.6. Predominant tagging of rhodopsin Cys^{140} or Cys^{316} with mBBr

Washed ROS membranes were incubated as above with a 20 fold molar excess of mBBr for only 5 min. Because of its higher reactivity, Cys^{316} of rhodopsin was primarily modified with mBBr under this short reaction time. The reaction was then terminated with the addition of a 100 fold molar excess of *N*-ethylmaleimide over rhodopsin [29].

Predominant labeling of Cys^{140} was achieved by blocking cysteine 316 with *N*-ethylmaleimide. For this, dark-depleted ROS membranes were initially incubated with a 20 fold molar excess of *N*-ethylmaleimide over rhodopsin, for 5 min, at 4 °C. Then, the excess label was eliminated by washing the modified ROS first with a 20 fold molar excess of L-cysteine in 5 mM Mes, 50 mM Hepes, and 1 mM EDTA (pH 6.7), and then with only buffer. Subsequently, the ROS sample was incubated with a 20 fold molar excess of mBBr over rhodopsin, as described above.

2.7. Digestion of rhodopsin with S. aureus V8 protease

Fluorescently labeled rhodopsin samples were digested with the V8 protease as described by Farrens et al. [30], using a rhodopsin:V8 protease ratio of 20:1 (w/w). After an overnight incubation, at room temperature, under constant agitation, the reaction was stopped by adding SDS-PAGE sample buffer [26], and the resulting fragments were analyzed by SDS-PAGE. After electrophoresis, the fluorescently labeled fragments were visualized using a transilluminator with a UV light. The V8 protease cleaves rhodopsin mainly at the C-terminal sides of Glu 239 and Glu 341 (Fig. 1) [30,31], and generates two fragments, F1 (~27 kDa), from the NH_2-terminal residue (Asn 2) to Glu 239, and F2 (~13 kDa), from Ser 240 to Glu 341. In addition, a heptapeptide containing the remaining carboxyl-terminal residues of rhodopsin is originated, (from Thr 342 to Ala 348). Since the larger F1 fragment contains Cys^{140} and the smaller F2 fragment contains Cys^{316}, the separation of the fragments in the gel provides evidence for the predominant labeling of each cysteine with mBBr.

2.8. Fluorescence excitation scans of mBBr-labeled rhodopsin samples

Fluorescence spectra were measured with a Hitachi F-7000 spectrofluorometer equipped with a Xenon lamp. Excitation scans were carried out from 300 to 450 nm, at 37 °C. The fluorescence emission was detected at 470 nm.

Before determining the corresponding fluorescence spectra, all samples of phosphorylated rhodopsin in ROS membranes were extensively washed with 5 mM Tris-HCl (pH 7.4), 2 mM EDTA, and 5 mM β-mercaptoethanol, in order to extract any new bound

peripheral proteins that were introduced with the enriched fraction of rhodopsin kinase.

Since all labeling reactions were performed on rhodopsin in ROS membranes, rhodopsin-containing samples were solubilized using 1% w/v *n*-dodecyl β-D-maltoside in 5 mM Mes, 50 mM Hepes, and 1 mM EDTA (pH 6.7) prior to assessing their fluorescence excitation spectra. References or blanks only contained the solubilization buffer [1% w/v *n*-dodecyl β-D-maltoside, 5 mM Mes, 50 mM Hepes, and 1 mM EDTA (pH 6.7)], and the resulting spectra were either subtracted from those of the corresponding rhodopsin-containing samples or shown as part of the graphs.

2.9. Other procedures

Protein concentration was determined according to Bradford [32], using bovine serum albumin as protein standard. SDS-PAGE was carried out on 1.5-mm thick slab gels containing 10 or 12% polyacrylamide [28]. The V8 proteolytic products of rhodopsin were separated by SDS-PAGE on 15% polyacrylamide gels. Because heat induces the formation of high-molecular weight rhodopsin aggregates, rhodopsin-containing samples were not boiled prior to SDS-PAGE. Coomassie blue R-250 was employed for the visualization of the polypeptide bands. For Western blot analyses, the proteins were electrotransferred from the gels to nitrocellulose filters [33]. Molecular distances between amino acid residues were calculated using the program Rasmol (version 2.7.1.1) on the crystal structures stored in the protein data bank (PDB, https://www.rcsb.org/pdb/home/home.do) for rhodopsin and metarhodopsin II (1U19 and 3PXO, respectively).

3. Results

The accessibility and reactivity of rhodopsin sulfhydryl groups were initially probed using three bimane derivatives, mBBr, dmBBr, and qmBBr. Although these compounds are originally non-fluorescent, the bimane-tagged materials exhibit high quantum yields of fluorescence when these derivatives react covalently with cysteine thiol groups [20,21]. All three fluorophores were capable of successfully modifying the native rhodopsin in its dark state, as shown by the fluorescently labeled band of 38 kDa that was obtained under UV illumination following SDS-PAGE separation (Fig. 2A). An additional low-migrating spot was observed under UV light when the gel was photographed immediately after the electrophoresis separation (Fig. 2A, arrowhead). Fig. 3A and B revealed that this spot probably resulted from the reaction between the remaining of the fluorophore and the β-mercaptoethanol contained in the sample buffer. It is atypical to find that a lower mobility spot than rhodopsin is attributed to the interaction of mBBr and β-mercaptoethanol, given that both are low molecular weight compounds. However, Tasheva and Dessev [34] have reported artifacts in SDS-PAGE due to the reducing agent present in the sample buffer. Specifically, β-mercaptoethanol seems to be responsible for the emergence of two non-protein bands with electrophoretic mobilities that correspond to about 68 and 54 kDa [34]. Therefore, it is not that rare to obtain a low-migrating spot produced by the reaction between mBBr and β-mercaptoethanol.

Similar fluorescence excitation spectra were obtained for samples of rhodopsin labeled with mBBr, dmBBr, and qmBBr (Fig. 2B). This figure shows that all fluorescently labeled rhodopsin samples possess an excitation maximum at about 375–380 nm. Since the highest fluorescence signal was acquired with mBBr, all the remaining procedures were carried out using mBBr as the modification reagent.

In theory, light activation causes changes in the conformational structure of the cytoplasmic loops of rhodopsin allowing transient

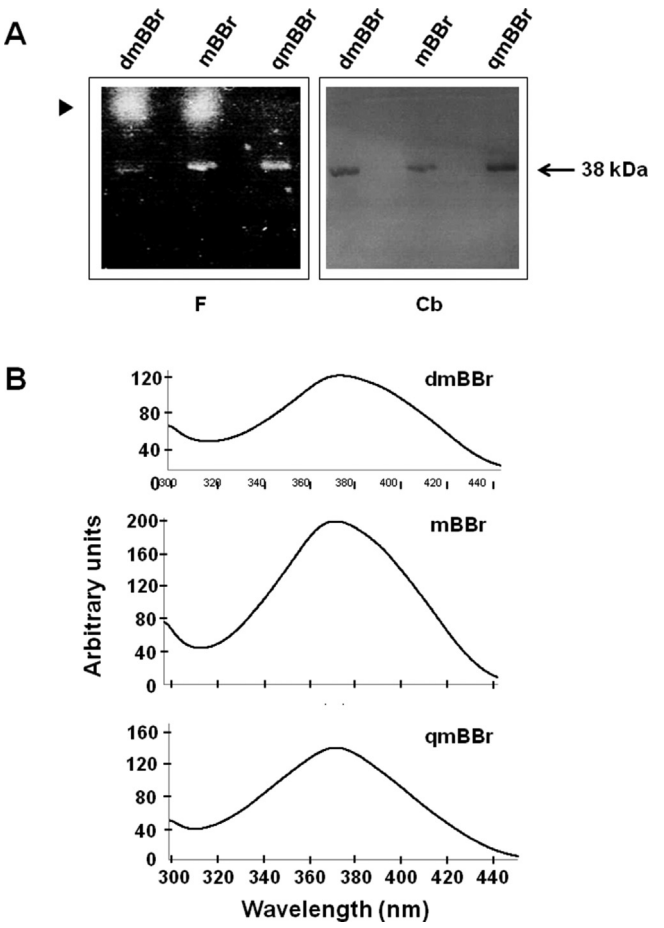

Fig. 2. Fluorescent labeling of rhodopsin with bimane derivatives. Washed ROS membranes were incubated in the dark with monobromobimane (mBBr), dibromobimane (dmBBr), or monobromotrimethylammoniobimane (qmBBr). ***A***, SDS-PAGE separation of the modified rhodopsin samples on a 12% polyacrylamide gel. The slab was immediately photographed under UV illumination to monitor fluorescence labeling (F), or stained for protein with Coomassie blue R-250 (Cb). The arrow indicates a polypeptide band of ~38 kDa that correspond to rhodopsin. A low-migrating fluorescent spot was also seen (arrowhead), which is generated by the reaction of the residual fluorophore and the β-mercaptoethanol contained in the sample buffer. ***B***, Fluorescence excitation spectra of rhodopsin labeled with mBBr, dmBBr, and qmBBr in the dark. In all cases, washed ROS membranes containing 0.15 mg of rhodopsin were employed.

recognition and binding of other signaling proteins of the visual cascade. Either dark or illuminated washed ROS membranes were incubated with mBBr, in order to evaluate whether the conformational changes that occur in light-activated rhodopsin hindered the labeling of the accessible cysteine residues. As seen in Fig. 3A and B, rhodopsin was equally labeled by mBBr in its dark and photolyzed state. It is known that rhodopsin possesses 10 cysteine residues, from which only Cys^{140} and Cys^{316} are available for chemical modification [8,9]. Moreover, V8 proteolysis of rhodopsin generates two fragments, F1 (~27 kDa, residues 1 to 239), and F2 (~13 kDa, residues 240 to 341) [30]. Since Cys^{140} and Cys^{316} are included in F1 and F2, respectively, fluorescently modified rhodopsin samples were digested with V8 to establish the labeling specificity. The degradation products F1 and F2 were analyzed by SDS-PAGE, and the fluorescent bands were identified by UV irradiation. As shown by V8 proteolysis, mBBr was capable of modifying both rhodopsin accessible cysteines, Cys^{140} and Cys^{316}, on both the inactive dark state and the light-activated state of the photoreceptor protein (Fig. 3A and B). A slow-migrating spot that resulted from the

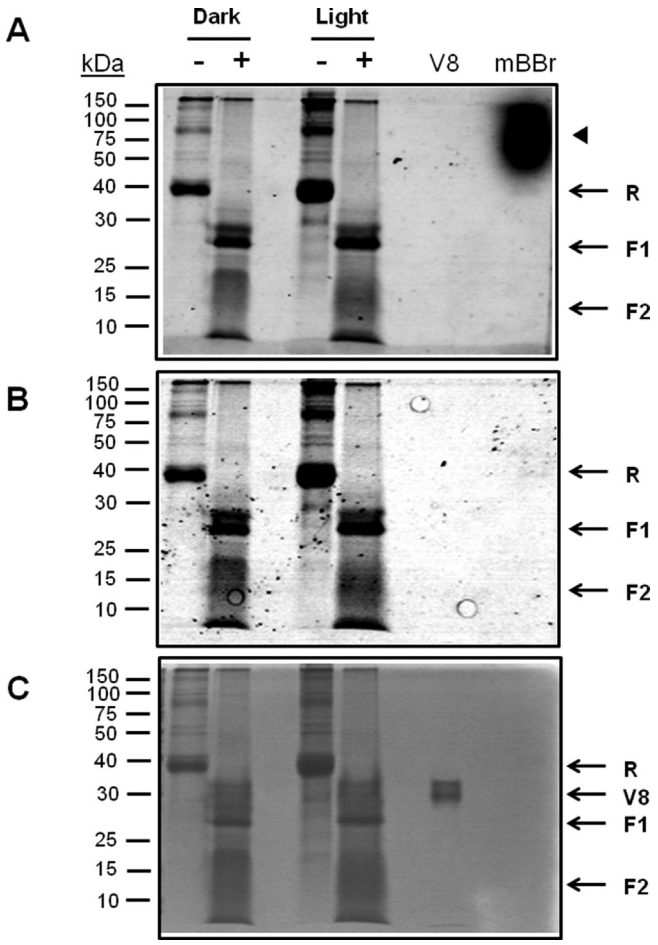

Fig. 3. Fluorescent labeling of inactive or light-activated rhodopsin at Cys^{140} and Cys^{316}. Dark or illuminated washed ROS membranes were incubated with mBBr. Fluorescently modified samples of the photoreceptor protein were digested (+) or not (−) with the V8 protease, and the resulting polypeptide bands were analyzed by SDS-PAGE. To monitor fluorescence labeling, the gel was immediately photographed (***A***) or photographed after a washing step with 25% isopropanol and 10% acetic acid (***B***) under UV illumination. Subsequently, the gel was stained for protein with Coomassie blue R-250 (***C***). Lanes containing samples of the V8 protease (V8) and monobromobimane alone (mBBr) were also included. Arrows indicate the migration of rhodopsin (R), the resulting proteolytic fragments F1 and F2, and V8. In ***A***, the arrowhead points to a low-migrating fluorescent spot that is generated by the reaction of mBBr and the β-mercaptoethanol contained in the sample buffer. This spot is eliminated after the washing step (***B***). SDS-PAGE separation was carried out on a 15% polyacrylamide gel.

reaction of mBBr with the β-mercaptoethanol contained in the sample buffer (Fig. 3A, arrowhead) was eliminated after washing the gel with 25% isopropanol and 10% acetic acid (Fig. 3B). Following fluorescence visualization by UV irradiation, the gel was stained for protein with Coomassie blue R-250 (Fig. 3C). As illustrated in Fig. 3C, the commercial V8 protease that possesses a molecular weight of 29,849 migrates as a doublet of ~30 kDa. As such, this doublet (29/31 kDa) was observed in all V8 protease digestion experiments and contaminated the lanes containing the rhodopsin F1 and F2 fragments.

Under illumination, rhodopsin can be phosphorylated by rhodopsin kinase on at least three sites located in its COOH-terminal region, Ser^{334}, Ser^{338} and Ser^{343} [15–18]. As seen by immunoblotting using anti-phosphoserine antibodies (Fig. 4A), rhodopsin in dark-depleted ROS membranes was phosphorylated in a light-dependent manner when an enriched fraction of rhodopsin kinase and Mg-ATP were used. No rhodopsin phosphorylation was attained when the reaction was performed in the dark (Fig. 4A). In this case, rhodopsin migrated as a band of ~35 kDa probably because the separation was carried out on a 10% polyacrylamide gel. Fig. 4B also illustrates that light-activated and phosphorylated rhodopsin was fluorescently labeled with mBBr, and both sites, Cys^{140} and Cys^{316} were modified given that both F1 and F2 were fluorescently tagged with mBBr (Fig. 4D). Therefore, the phosphorylation of the exposed serine residues did not affect the labeling of these cysteines with mBBr. Moreover, prior labeling of the Cys^{140} and Cys^{316} with mBBr did not hinder the phosphorylation of the C-terminal tail Ser/Thr residues (Fig. 4C).

By a proper choice of the reaction conditions, either Cys^{140} or Cys^{316} of rhodopsin could be predominantly labeled with mBBr (Fig. 5A). The most reactive cysteine (Cys^{316}) was primarily labeled with mBBr when the reaction was carried out for only 5 min. In this case, the F2 fragment containing Cys^{316} was preferentially modified (~80–85%) following digestion with the V8 protease, despite the fact that some fluorescent F1 was also obtained (~15–20%) corresponding to a minor amount of contaminating mBBr-labeled Cys^{140} (Fig. 5A). To label Cys^{140} selectively, Cys^{316} was first quantitatively blocked by reaction with an excess of *N*-ethylmaleimide for a short reaction time. Cys^{140} was then fluorescently modified under conditions of high molar excess of mBBr to rhodopsin. Proteolytic digestion with V8 protease revealed that of the two fragments only F1 was fluorescent (Fig. 5A), proving evidence that only Cys^{140} was modified with mBBr. Although the amount of the mBBr-modified F1 band appears to be similar under both conditions (Fig. 5A), the effect of the contaminating mBBr-modified Cys^{140} on the fluorescence excitation signal of the protein containing predominantly the mBBr-labeled Cys^{316} should be negligible. Moreover, since the fluorescence signal is measured by arbitrary units, the small amount of mBBr-labeled Cys^{140} is sufficient for the case where only this cysteine is selectively modified with the fluorophore. Following fluorescence visualization by UV irradiation, the gel was stained for protein with Coomassie blue R-250 (Fig. 5B). As shown before, the V8 protease migrated as a doublet of ~30 kDa, which contaminated the lanes containing the rhodopsin F1 and F2 fragments (Fig. 5B). In addition, rhodopsin samples that were mainly modified with mBBr at Cys^{316} or Cys^{140} were successfully phosphorylated by rhodopsin kinase (data not shown).

As control experiments, fluorescence spectra were initially determined on the unmodified rhodopsin in its dark, light-activated, or illuminated and phosphorylated states. As shown in Fig. 6, these samples did not show any intrinsic fluorescence signals throughout the range utilized to scan the excitation of the labeled proteins (i.e. between 300 and 440 nm). However, two excitation peaks were detected at about 237 nm and 470 nm in the three samples (Fig. 6), which probably correspond to the intrinsic fluorescence excitation signals of the protein aromatic residues and the retinal chromophore, respectively. Interestingly, both peaks showed downfield shifts compared to their regular maxima, indicating that the aromatic residues and retinal are buried and probably interacting with other groups or moieties within the protein. It is known, for example, that the fluorescence of the 5 tryptophans of rhodopsin is quenched by their close proximity to the retinal chromophore in its three dimensional structure [35]. Additionally, fluorescence excitation spectra were monitored individually for L-cysteine and mBBr, and neither of these compounds possesses intrinsic fluorescence in the range that was evaluated. However, when L-cysteine was reacted with mBBr, the resulting reaction product was highly fluorescent, showing an excitation peak at about 335 nm (data not shown).

Fluorescence spectra were measured following rhodopsin

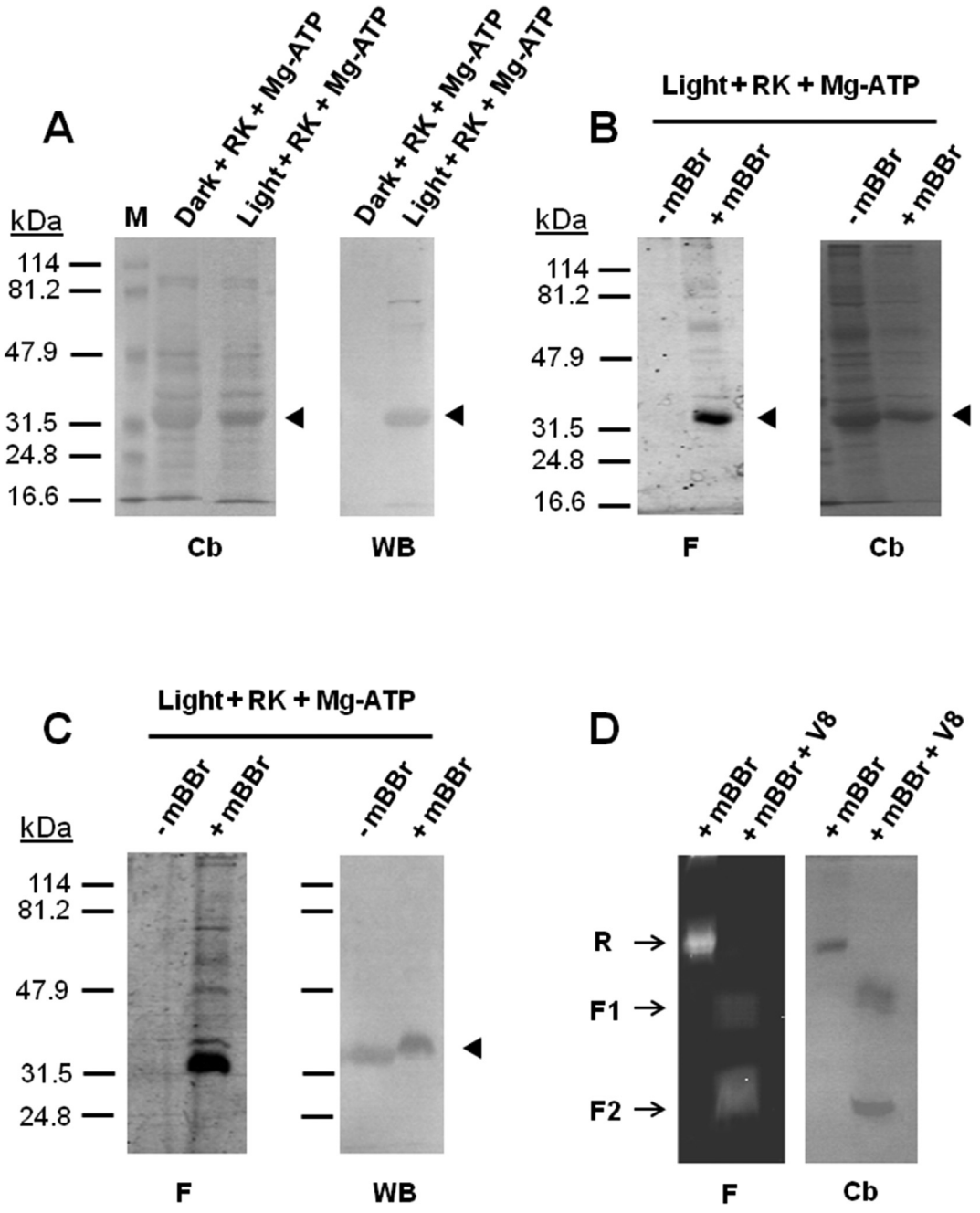

Fig. 4. Labeling with mBBr of photoactivated and phosphorylated rhodopsin at Cys^{140} and Cys^{316}. ***A***, Rhodopsin in washed ROS membranes was phosphorylated in a light-dependent manner using an enriched fraction of rhodopsin kinase (RK), in the presence of Mg-ATP. M = molecular weight markers. ***B***, Photoactivated and phosphorylated rhodopsin was fluorescently labeled with mBBr. A sample of unlabeled rhodopsin is included (- mBBr). ***C***, mBBr-labeled rhodopsin in the dark was phosphorylated by RK following illumination. A sample of unlabeled rhodopsin is included (- mBBr). ***D***, Light-activated and phosphorylated rhodopsin was labeled at Cys^{140} and Cys^{316} given that both fragments, F1 and F2, were fluorescently tagged with mBBr following digestion with the V8 protease (V8). Arrows indicate the migration of rhodopsin (R) and the proteolytic fragments F1 and F2. Cb = Coomassie blue R-250 staining, WB = western blotting using anti-phosphoserine antibodies, F = fluorescence labeling under UV illumination. In ***A***, ***B*** and ***C***, SDS-PAGE separation was carried out on 10% polyacrylamide gels; in ***D***, SDS-PAGE separation was carried out on a 15% polyacrylamide gel.

labeling with mBBr in its dark and photoactivated states. Interestingly, only a minor shift of <1 nm in the wavelength of the maximum fluorescence excitation peak was observed when both samples were compared (Fig. 7A). These results demonstrated that the light-induced conformational changes of photoactivated rhodopsin cannot be probed by fluorescent labeling with mBBr at Cys^{140} and Cys^{316}. It is known that the fluorescence emitted by most molecules is extremely sensitive to their microenvironment. It appears that the chemical microenvironment in close proximity to the mBBr-modified cysteines of rhodopsin remains unaltered in the dark and light-activated states of the photoreceptor protein. In contrast, the intensity of the fluorescence signal decreased ~90% when rhodopsin was light-activated and then phosphorylated (Fig. 7A). For comparison, an experiment was also performed by first phosphorylating the photoactivated rhodopsin, and then subjecting the sample to labeling with mBBr at both cysteines (Fig. 8). In this case, the initial fluorescence peak obtained for the mBBr-labeled sample also decreased ~90% when the sample was

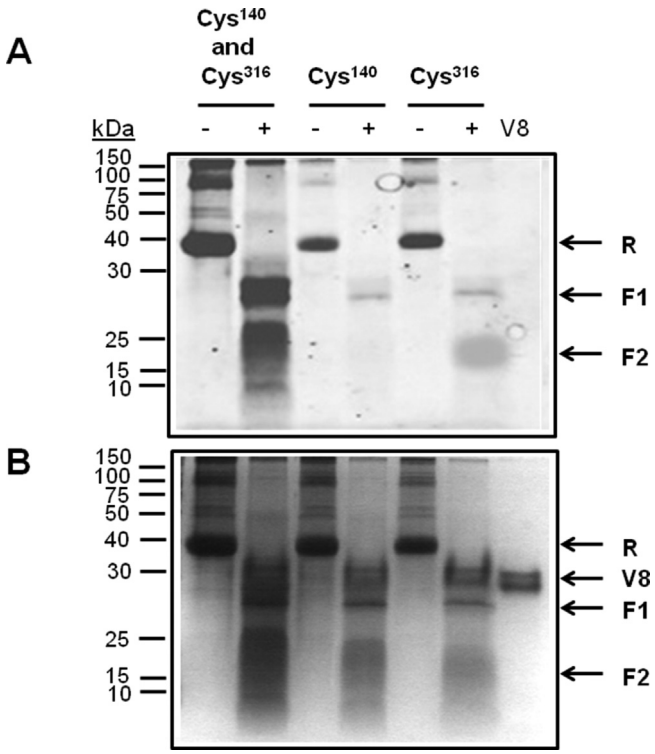

Fig. 5. Site-specific modification of rhodopsin Cys^{140} or Cys^{316} with mBBr. Dark-depleted ROS membranes were incubated in the dark with mBBr for 16 h, to label both accessible rhodopsin cysteines (Cys^{140} and Cys^{316}). Rhodopsin Cys^{316} was selectively modified by incubating washed ROS membranes with mBBr in the dark for just 5 min (Cys^{316}). Site-specific labeling of rhodopsin Cys^{140} was achieved by blocking rhodopsin Cys^{316} with *N*-ethylmaleimide for 5 min, and then the washed ROS sample was incubated in the dark with mBBr for 16 h (Cys^{140}). Fluorescently modified samples of rhodopsin were digested (+) or not (−) with the V8 protease, and the resulting polypeptide bands were analyzed by SDS-PAGE. To monitor fluorescence labeling, the gel was photographed after a washing step with 25% isopropanol and 10% acetic acid (***A***) under UV illumination. Afterward, the gel was stained for protein with Coomassie blue R-250 (***B***). A lane containing a sample of the V8 protease (V8) was included. Arrows indicate the migration of rhodopsin (R), the resulting proteolytic fragments F1 and F2, and V8. SDS-PAGE separation was carried out on a 15% polyacrylamide gel.

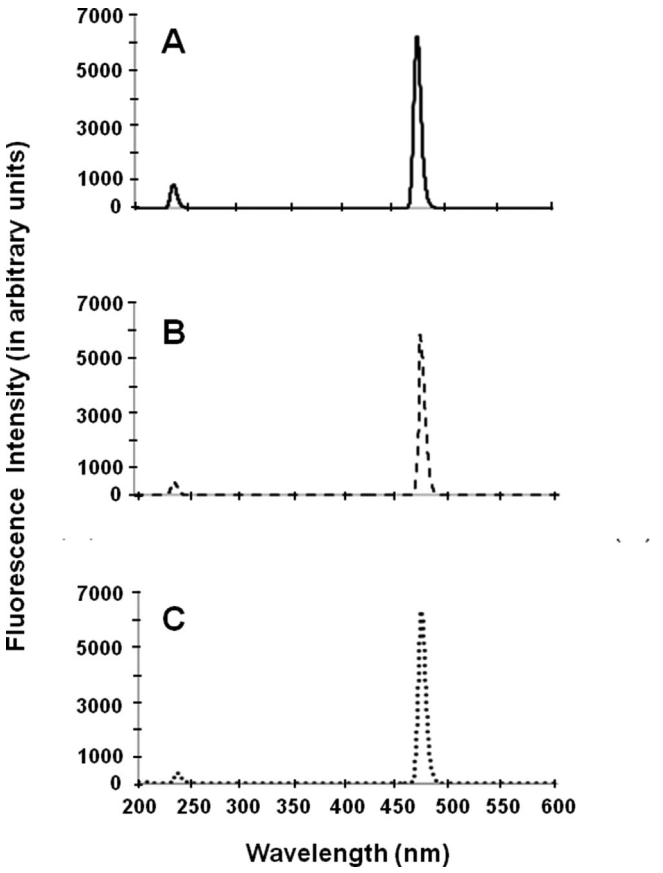

Fig. 6. Fluorescence excitation spectra of unlabeled rhodopsin in its dark, light-activated, or illuminated and phosphorylated states. The intrinsic fluorescence of free rhodopsin in dark-depleted ROS membranes was determined in its ground (***A***), photoactivated (***B***) or illuminated and phosphorylated (***C***) states. Excitation scans were carried out from 200 to 600 nm, at 37 °C.

initially phosphorylated.

Given that we are using dark-depleted ROS membranes and an enriched fraction of rhodopsin kinase instead of using purified proteins, it is plausible to consider that the loss of fluorescence in phosphorylated rhodopsin could be caused by the binding of other retinal proteins once rhodopsin is phosphorylated. If that is the case, the specific interaction of eventual proteins to phosphorylated rhodopsin might produce the quenching reported here. However, in all the phosphorylation experiments, we mixed 50 μg of rhodopsin as dark-depleted ROS membranes, and 10 μg of total protein in the fraction containing the partially purified rhodopsin kinase. Since the main protein component of the ROS disk membranes is rhodopsin (>90%) [1], the amount of rhodopsin kinase, transducin and arrestin-1 in the rhodopsin kinase-enriched fraction was sub-stoikiometric and almost irrelevant when compared to the significant amount of rhodopsin present in the reaction mixtures. It is also crucial to keep in mind that prior to the measurement of the fluorescence excitation spectra, the samples of phosphorylated rhodopsin in the ROS membrane samples were extensively washed with hypotonic buffer to promote the release of any potential interacting proteins that were introduced with the fraction that contained the partially purified rhodopsin kinase.

In order to determine whether there was any quenching effect produced by the other protein components present in the partially purified rhodopsin kinase fraction, we also performed the following additional experiments as controls: i) a sample of rhodopsin in dark-depleted ROS membranes was modified with mBBr, and then was incubated with the enriched fraction of rhodopsin kinase in the dark and in the presence of Mg-ATP (Fig. 9A), ii) a sample of mBBr-labeled rhodopsin in dark-depleted ROS membranes was illuminated in the presence of Mg-ATP but without the addition of the enriched fraction of rhodopsin kinase (Fig. 9B), and iii) a sample of mBBr-labeled rhodopsin in dark-depleted ROS membranes was just illuminated in the presence of the enriched fraction of rhodopsin kinase but in the absence of Mg-ATP (Fig. 9C). Following extensive washes with hypotonic buffer, the fluorescence excitation spectrum of each sample was measured. As seen in Fig. 9, these three control samples showed comparable excitation spectra with similar peaks at about 375–380 nm, and no quenching was revealed by the presence of the partially purified rhodopsin kinase fraction. Moreover, no fluorescence signal was seen when the spectra of the references were measured (Fig. 9). Therefore, the loss of the fluorescence signal seen above (Figs. 7A and 8) must be generated by conformational changes induced in rhodopsin after its phosphorylation.

Fluorescence spectra were also determined on rhodopsin samples that were predominantly labeled at either Cys^{140} or Cys^{316}, and then phosphorylated, in an attempt to identify which of the two mBBr-labeled cysteines was responsible for the decrease in the fluorescence signal of the photolyzed phosphorhodopsin. For the rhodopsin sample that was selectively labeled with mBBr on Cys^{140},

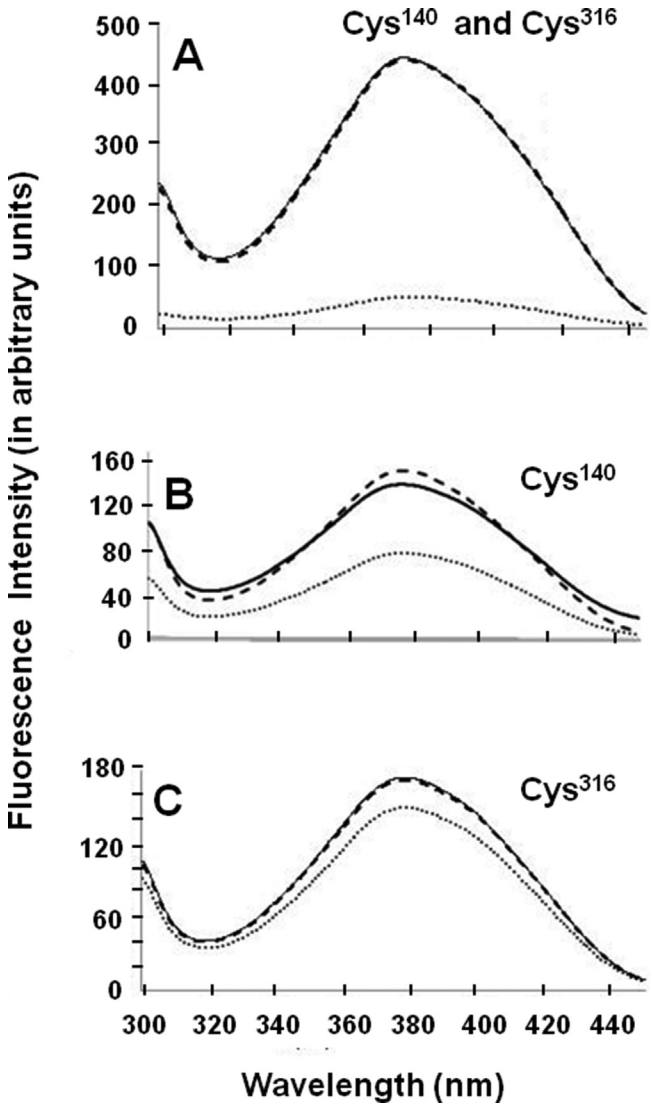

Fig. 7. Fluorescence excitation spectra of rhodopsin labeled with mBBr in its inactive, photoactivated, or photoactivated and phosphorylated states. Samples of rhodopsin in washed ROS membranes were labeled with mBBr in the dark. Shown are samples of the protein modified at both cysteine residues (Cys^{140} and Cys^{316}), or selectively labeled at either residue 140 (Cys^{140}) or 316 (Cys^{316}). Aliquots of these samples were directly used or subjected to either light-activation or light-dependent phosphorylation. Dark state (continuous line), light-activated state (- - -), photoactivated and phosphorylated state (·····).

almost no change was observed in the fluorescence excitation spectra of the inactive and light-activated rhodopsin (Fig. 7B). Similar results were obtained for the rhodopsin sample that was predominantly labeled with mBBr on Cys^{316} (Fig. 7C). On the contrary, the intensity of the fluorescence signal for the rhodopsin samples that were primarily labeled with mBBr on either Cys^{140} or Cys^{316} decreased ~38% and 28%, respectively, when the photoreceptor protein was light-activated and phosphorylated (Fig. 7B and C). None of the phosphorylated samples generated a decrease of ~90% in the original fluorescence signal. These results demonstrated that the effect caused by phosphorylation on the fluorescence of the labeled protein cannot be attributable to the modification of only one of the cysteine residues. Moreover, the effect did not appear to be additive but synergistic.

The chemical composition of the phosphoryl group confers upon any phosphorylated protein certain additional

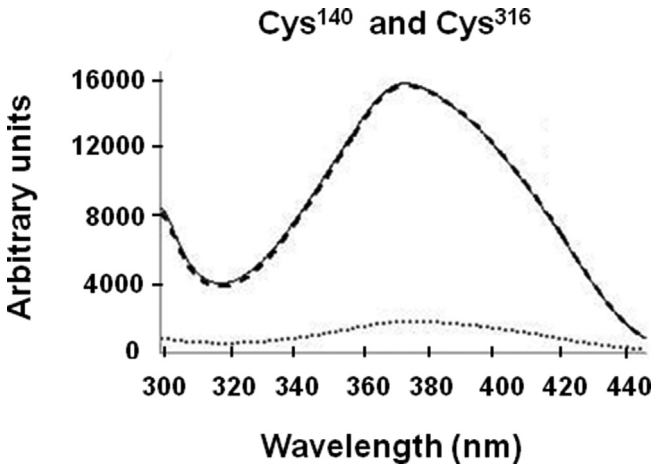

Fig. 8. Fluorescence excitation spectra of photoactivated phosphorhodopsin that was subsequently labeled with mBBr. Rhodopsin in washed ROS membranes was first photoactivated and phosphorylated, and then modified with mBBr at both cysteine residues (Cys^{140} and Cys^{316}). As a control, samples of dark and illuminated rhodopsin were also modified with mBBr at Cys^{140} and Cys^{316}. Dark state (continuous line), light-activated state (- - -), photoactivated and phosphorylated state (·····).

characteristics that affect the structural, thermodynamic and kinetic properties of the phosphorylated protein. In particular, each phosphate group that is incorporated adds two negative charges to the protein, modifying and disrupting the initial electrostatic interactions, and generating potential structural changes in the protein tridimensional fold. Our results clearly demonstrated that the phosphorylation of Ser/Thr residues on the rhodopsin C-terminal tail induced an important conformational change in the photoreceptor protein, which can be probed by mBBr labeling at Cys^{140} and Cys^{316}. These findings may suggest that the C-terminal tail containing the phosphorylated hydroxyl groups might be positioned relatively close to the cytoplasmic surface of the protein where both mBBr-modified cysteines are located. Since mBBr is very sensitive to its immediate surroundings and polar environments are capable of quenching the fluorescence of mBBr-labeled cysteines, fluorescence quenching may occur if as a result of the phosphorylation-induced conformational changes of rhodopsin, its carboxyl-terminal tail is rearranged in such a way that the negatively charged phosphoryl groups are relocated into a position in close proximity to the mBBr-tagged cysteines. Computational analyses using the crystal structure of meta-rhodopsin II that corresponds to photoactivated rhodopsin, was employed to determine the distances between each of the sulfurs at the sulfhydryl groups of Cys^{140} and Cys^{316} and each of the hydroxyl groups of Ser^{334}, Ser^{338} and Ser^{343}, which are the predominant phosphorylation sites. We noticed that Cys^{316} is relatively close to the three serine residues (<10.5 Å), which partially might account for the decrease in fluorescence intensity. However, Cys^{140} is far from the phosphorylated serines (>22 Å), making it unfeasible for the incorporated phosphoryl groups to influence the fluorescence signal of the labeling fluorophore. In addition, the fluorescence signal of the mBBr-modified rhodopsin was not altered in the presence of various concentrations of sodium phosphate, either in the dark (Fig. 10) or following illumination (data not shown). Moreover, phosphate groups have not been previously reported to act as fluorescence quenchers. Therefore, we believe that the incorporated phosphate groups are not responsible of the quenching. It is more likely that buried amino acid residues in rhodopsin become available after illumination and phosphorylation, quenching in turn the fluorescence excitation signal of mBBr-labeled rhodopsin.

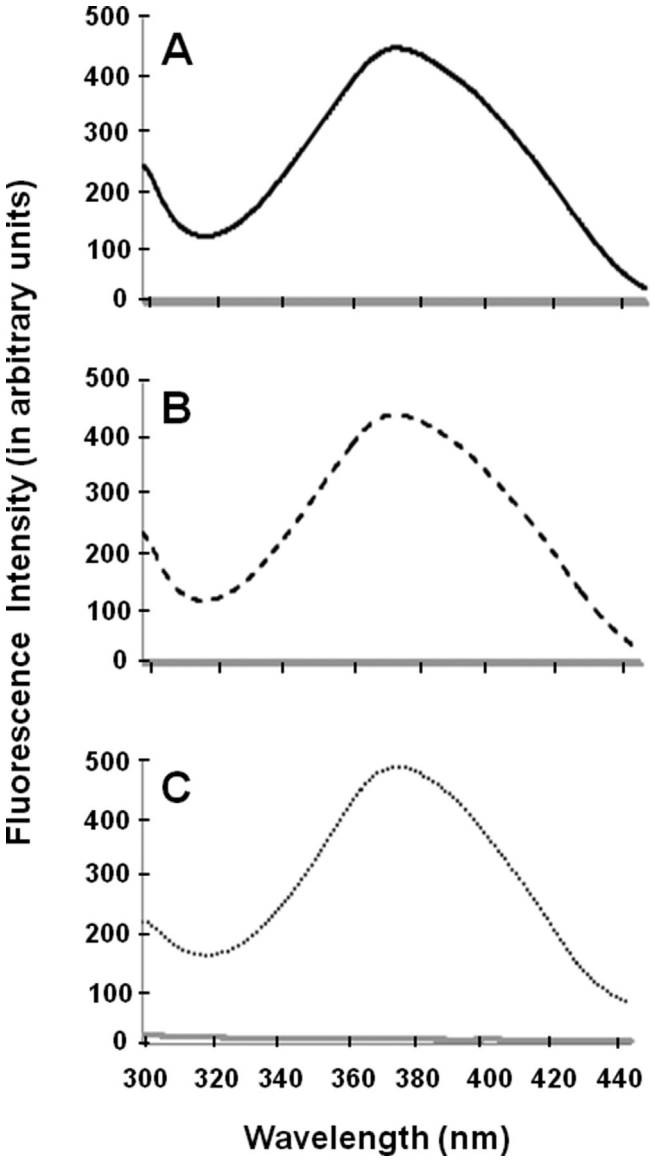

Fig. 9. No fluorescence quenching was seen following incubation of mBBr-labeled rhodopsin with the partially purified rhodopsin kinase fraction. ***A***, Rhodopsin in dark-depleted ROS membranes was modified with mBBr, and then incubated with the enriched fraction of rhodopsin kinase in the dark and in the presence of Mg-ATP. ***B***, mBBr-labeled rhodopsin in dark-depleted ROS membranes was illuminated in the presence of Mg-ATP but without the addition of the enriched fraction of rhodopsin kinase. ***C***, mBBr-labeled rhodopsin in dark-depleted ROS membranes was just illuminated in the presence of the enriched fraction of rhodopsin kinase but in the absence of Mg-ATP. Fluorescence excitation spectra were measured after extensive washes of the samples with hypotonic buffer. The gray solid line included in each graph represents the spectra of the corresponding blank containing just the solubilization buffer [1% w/v *n*-dodecyl β-D-maltoside, 5 mM Mes, 50 mM Hepes, and 1 mM EDTA (pH 6.7)].

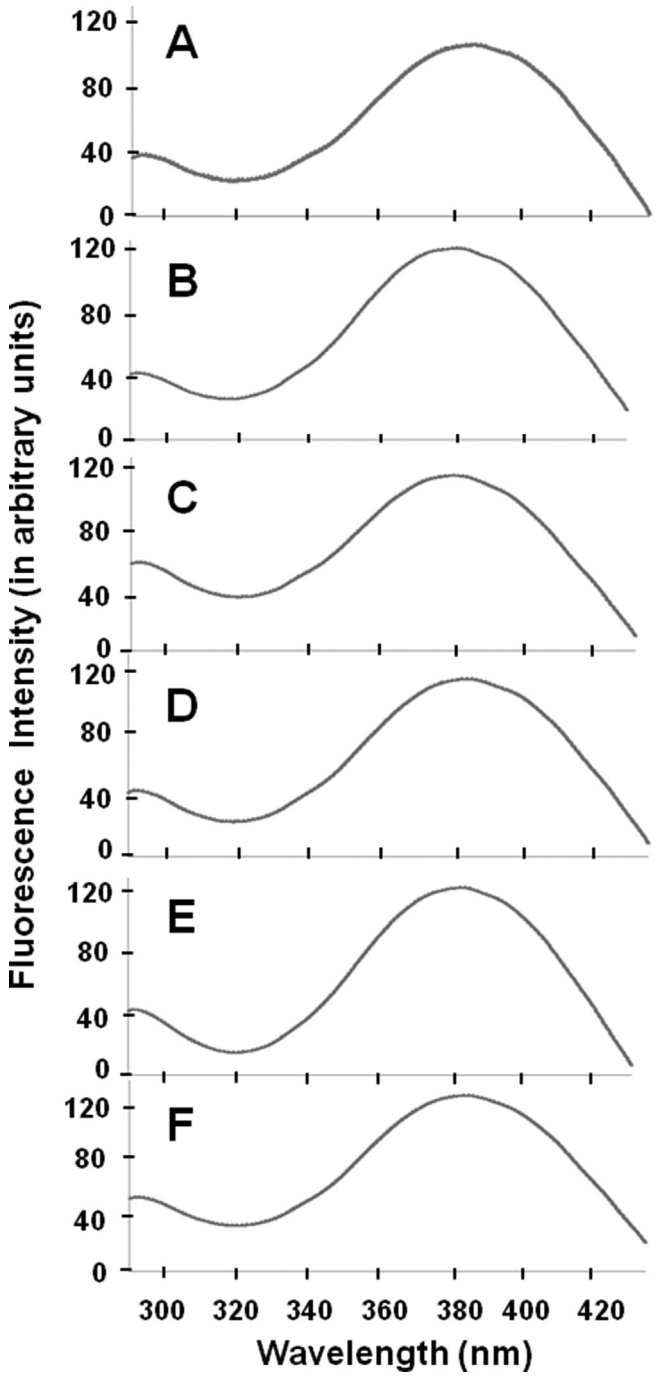

Fig. 10. Fluorescence excitation spectra of mBBr-modified rhodopsin in the presence of various concentrations of sodium phosphate. Samples of rhodopsin in washed ROS membranes were labeled with mBBr in the dark. Fluorescence spectra were monitored in the presence of 50 mM (***A***), 100 mM (***B***), 200 mM (***C***), 300 mM (***D***), 400 mM (***E***) or 500 mM (***E***) sodium phosphate.

4. Discussion

We used mBBr to modify the thiol groups of the accessible rhodopsin cysteines, Cys^{140} and Cys^{316}, in order to analyze conformational changes taking place following light-activation and phosphorylation of the protein. Both cysteines are located at the cytoplasmic side of rhodopsin; Cys^{140} is the first residue in the C2 loop, and Cys^{316} is at the middle of the amphipathic helix VIII (Fig. 1). Interestingly, the C2 loop is positioned at the cytoplasmic termination end of transmembrane helix 3 that contains the Glu^{113} counterion, and helix VIII is situated after transmembrane helix 7 that contains the Lys^{296} bound to the 11-*cis*-retinal chromophore via a protonated Schiff base linkage. In the ground state this positive charge is stabilized by the counterion Glu^{113}. Upon activation and metarhodopsin II formation, this salt bridge is broken, which theoretically removes a structural constraint between helices 3 and 7. However, when fluorescence spectra were compared between samples of mBBr-tagged rhodopsin under dark and light conditions, no effect on the fluorescence signal was perceived and only a minor shift of <1 nm was observed in the wavelength values of the

excitation maxima. Hence, no major alterations in conformation after light exposure of rhodopsin were detected by fluorescence excitation scans of the mBBr-labeled protein. Similar results were obtained with rhodopsin samples that were predominantly labeled at either Cys^{140} or Cys^{316}, showing no variation between the fluorescence excitation spectra of the inactive and light-activated site-specific mBBr-labeled rhodopsins. Our results are consistent with the X-ray diffraction structural findings of Choe et al. [36] that reported that transmembrane helices 1, 2, 3, 4 and 7, as well as amphipathic helix VIII, suffer little changes following rhodopsin activation. On the other hand, transmembrane helices 5 and 6 are the regions where the most significant structural alterations take place when the crystal structures of the inactive and light-activated forms of rhodopsin are compared [36].

Most previous reports showing light-dependent changes in the fluorescence of rhodopsin have not used the approach that we employed here. For instance, Imamoto et al. [8] incubated rhodopsin in native membranes with Alexa594-maleimide, which allowed them to monitor fluorescence changes at a wavelength of 605 nm. An increase in fluorescence intensity of ~20% was reported following illumination of the Alexa594-labeled rhodopsin [8]. In addition, Mielke et al. [9] modified rhodopsin Cys^{140} and Cys^{316} with fluorescein and Texas Red by using 5-iodoacetamidofluorescein and C_5-bromoacetamido Texas Red, respectively. Measurements of the time-resolved fluorescence depolarization were carried out both in the ground dark state and in the photoactivated state of the fluorescently-labeled proteins, showing significant differences. Specifically, a large decrease in motional freedom was observed after illumination, which indicated increased steric hindrance in the rhodopsin light-activated state [9]. Interestingly, all three extrinsic fluorophore dyes, Alexa594, fluorescein and Texas Red, are larger in size than monobromobimane. Since they occupy a greater space within the protein, all three fluorescent labels may produce subtle folding alterations close to the sites at which they are covalently bound, yielding, in turn, measurable changes in their fluorescence signals. In contrast, the fluorescent moiety of mBBr is small since it is only formed by two pentacyclic rings, and as such, this compound provide minimum of opportunity for perturbation of the protein conformation near those sites at which they are covalently bound. Perhaps, for that reason, no evident changes in the fluorescence signal of mBBr-labeled rhodopsin were detected upon photoactivation. Comparable mBBr labeling experiments as those presented here, were performed on rhodopsin constructs that contain specific residues replaced by cysteines [37], but surprisingly similar type of experiments were not carried out on the wild-type or native protein. In fact, most work involving labeling of rhodopsin with fluorophores utilizes site-directed fluorescence labeling. For example, mBBr-labeling followed by fluorescence spectroscopic analysis showed that the excitation spectra of the fluorescently-labeled rhodopsin mutant V250C exhibited a downfield or blue shift in its λ_{max} of about 5–6 nm, indicating that the label at this position became more hydrophobic following light-activation [37]. Labeling with PyMPO-maleimide, another cysteine-specific modification reagent, confirmed their findings [37]. Since Val^{250} is located on the inner face of rhodopsin transmembrane helix 6, their results provided direct evidence that rhodopsin activation involves a conformational change in this region of the protein.

We also showed that the labeling of Cys^{140} and Cys^{316} with mBBr did not thwart the phosphorylation of rhodopsin by rhodopsin kinase; moreover, the phosphorylation of the hydroxyl groups at the C-terminal tail of rhodopsin did not prevent the labeling of both cysteine residues. These results are interesting, given that Krupnick et al. [38] have shown that rhodopsin phosphorylation hindered and decrease transducin binding promoting high-affinity arrestin binding and allowing arrestin to effectively compete with transducin for binding to photoactivated rhodopsin. Probably, the effect on transducin binding when rhodopsin is phosphorylated is generated by polar repulsion rather than by steric hindrance.

Strikingly, the fluorescence signal was highly reduced (~90%) in samples containing photoactivated and phosphorylated mBBr-labeled rhodopsin at both cysteines. However, predominant site-specific fluorescent labeling of light-activated phosphorhodopsin at either Cys^{140} or Cys^{316} only produced a fair decrease of ~38% and 28%, respectively, in the intensity of its fluorescence signal, demonstrating that the phosphorylation effects are not due to the modification of a particular cysteine. Since the outcome detected in mBBr-labeled photoactivated phosphorhodopsin at both cysteines was not mimicked by adding the effects of each site-specific mBBr-labeled phosphorhodopsin, we assumed that the effect acquired in photoactivated phosphorhodopsin fluorescently tagged at Cys^{140} and Cys^{316} was not additive but synergistic and cooperative.

Suitable selection of the reaction conditions allowed us to predominantly modify with the mBBr probe either Cys^{140} or Cys^{316}. However, when the reaction was performed with the purpose of modifying only Cys^{316}, some contamination of ~15–20% with mBBr-labeled Cys^{140} was attained. A clear-cut strategy to avoid labeling contaminations would have been to generate rhodopsin mutants carrying single Ser or Ala replacements at the position of the two reactive cysteines. As a future recommendation, it will be interesting to work with this Cys to Ser (or Ala) site-specific constructs in order to prevent potential overlapping of the fluorescence signals and to confirm our findings.

It is mostly certain that by using the experimental strategy designed here, there is an incomplete labeling of the protein, especially in those cases when one of the Cys is predominantly modified with mBBr. Therefore, the concentration of the covalently bound fluorophore might be lower when one of the Cys is primarily labeled with mBBr. Accordingly, the fluorescence signals of the samples in which the protein was predominantly labeled at either Cys^{140} or Cys^{316} were inferior than the signal observed when both cysteines were modified with the fluorescent compound at the same time. For testing the functionality of a fluorophore-labeled protein, a labeling stoichiometry close to 100% is mandatory [35,40]. Yet, we are not testing here the functionality of the mBBr-labeled rhodopsin, and as such, the concentration of the modified rhodopsin should not be a concern. It is known that low labeling stoichiometry can be used for most fluorescent studies, and is even required when working with membranes and performing anisotropy studies to prevent homo-energy transfer between nearby fluorescent probes. Therefore, a lower incorporation of the mBBr fluorophore in those cases where one of the Cys is predominantly modified, should not affect the fluorescence quenching because the generation of the dark-state, light-activated state, and illuminated and phosphorylated state of rhodopsin is independent of the amount of mBBr being incorporated into the protein and only depends on the presence or absence of light and the appropriate conditions that induce the phosphorylation of rhodopsin.

It is plausible that there is some lipid reorganization when photoactivated phosphorhodopsin is generated in the ROS membranes, and that lipids in the membrane may quench the signal. It is known that the lipid composition of ROS disks is highly specialized, containing a large fraction of polyunsaturated fatty acids, particularly docosahexaenoic acid [41,42]. Interestingly, the reconstitution of rhodopsin in model membranes has revealed that the functional activity of the photoreceptor protein is enhanced by the incidence of docosahexaenoic acid acyl chain-enriched phospholipids [43–45], and this effect was improved by the presence of phosphatidylethanolamine [46]. In contrast, the inactive ground state of rhodopsin is stabilized by cholesterol [47]. Also, it has been

reported that rhodopsin is sensitive to bilayer thickness, lipid packing, membrane order, and curvature elastic stress [48]. Since docosahexaenoic acid is known to lower the packing density and order of lipid membranes, it probably facilitates the conformational transitions that lead to the photoactivated state of the protein. On the other hand, cholesterol likely counteracts these effects by ordering the membrane and increasing its thickness. In addition, docosahexaenoic acid and phosphatidylethanolamine are non-lamellar-phase-forming lipid components and introduce negative curvature elastic stress in membranes. By dynamics simulations, Salas-Estrada et al. [49] have shown that a local ordering effect appeared to take place in the membrane upon changes that are induced in the rhodopsin structure following activation. Likewise, docosahexaenoic acid acyl tails and phosphatidylethanolamine headgroups behaved like weak ligands, preferentially binding to rhodopsin in inactive-like conformations and inducing subtle but significant structural changes [49]. On the basis of all these observations, the light-activation of rhodopsin in lipid bilayers seems to be influenced by the composition of its lipidic environment, and concomitantly, there appear to be alterations in lipid bilayers after rhodopsin activation. Thus, the quenching of the fluorescence signal reported here could be produced by lipid reorganization in the membrane, but if that is the case, it may seem likely that the lipid reorganization is a direct consequence of the conformational change caused by the phosphorylation of Ser/Thr residues on the C-terminal region of photoactivated rhodopsin.

Since we showed that the fluorescence signal of the mBBr-modified rhodopsin was not modified in the presence of increasing concentrations of sodium phosphate, it seems unlikely that the incorporated phosphate groups are responsible of the observed quenching. Alternatively, our findings can be justified by additional conformational changes that may take place as a consequence of rhodopsin photoactivation and phosphorylation. If this is the case, residues that are good fluorescence quenchers, and are probably buried in the dephosphorylated state of the photoreceptor protein, are capable of becoming accessible to reach the vicinity of the mBBr-modified cysteines decreasing in turn their signal intensity. It is known that bimane fluorescence can be quenched by tryptophan and, to a lesser extent, tyrosine side chains in proteins [50–52]. This quenching occurs through an excited-state electron transfer mechanism that requires close proximity between the bimane fluorophore and the aromatic side chain, with a sphere of quenching on the order of $\leq$10 and 15 Å for Tyr and Trp, respectively [50,52]. Hence, it is possible that aromatic side chains that are buried in the interior of the three-dimensional structure of both the dark and the illuminated states of rhodopsin, become accessible and proximal to the mBBr-labeled cysteines, following the conformational changes that are induced by phosphorylation on photoactivated rhodopsin, and, in consequence, these side chains will generate position-specific fluorescence quenching.

Various reports attempting to elucidate the structure of the COOH-terminal tail of rhodopsin containing the phosphorylation sites have been published. The structure of a peptide that corresponds to the last 19 residues of bovine rhodopsin (residues 330–348), containing various number of phosphates, was determined by using two-dimensional NMR [53]. This study showed little ordering of the peptide upon phosphorylation; however, Kisselev et al. [54] have shown by NMR that although this peptide is completely disordered in solution, it becomes structured upon binding to arrestin-1. Consistently, Getmanova et al. [55] have reported by using NMR spectroscopy that the phosphorylated C-terminus is highly mobile in the intact mammalian photoreceptor rhodopsin. Interestingly, binding of the fully phosphorylated polypeptide, representing the last 19 residues of bovine rhodopsin, to arrestin-1, leads to the peptide folding into a helix-loop structure [56]. No three-dimensional structure of the photoactivated phosphorhodopsin is yet available; however, the crystal structure of a constitutively active form of rhodopsin bound to a pre-activated form of arrestin-1 was determined by serial femtosecond X-ray laser crystallography [57]. The structure reveals an overall architecture of the rhodopsin-arrestin-1 assembly in which rhodopsin uses distinct structural elements, including transmembrane helix 7 and the amphipatic helix VIII, to recruit arrestin-1. Correspondingly, arrestin-1 adopts the pre-activated conformation, which opens up a cleft in the protein to accommodate a short helix formed by the C2 loop of rhodopsin. While seven-transmembrane-helix receptors undergo major conformational changes in their intracellular pockets from an inactive to an active state, the differences in conformation between a G protein-bound state and an arrestin-bound state are relatively small [58]. However, some dissimilarities have been found, such as the larger outwards movement of the C-terminal half of helix 6 and the slightly larger intracellular pocket in the G protein bound receptor. Yet, the phosphorylation and the conformational change in the C-terminal tail of these receptors are specific for arrestin recruitment. Recently, Zhou et al. [59] have reported that the phosphorylated C terminus of rhodopsin forms an extended intermolecular β sheet with the N-terminal β strands of arrestin-1. Phosphorylation was detected at rhodopsin C-terminal tail residues Thr^{336} and Ser^{338}, and these two phosphoresidues, together with Glu^{341}, form an extensive network of polar interactions with three positively charged pockets formed by three groups of basic residues in arrestin-1. All these findings are consistent with the phosphorylation-induced conformational changes of light-activated rhodopsin that have been probed here by fluorescent modification at Cys^{140} and Cys^{316}.

5. Conclusions

By using fluorescent labeling with monobromobimane at Cys^{140} and Cys^{316}, we demonstrated that the phosphorylation of Ser/Thr residues on the C-terminal region of photoactivated rhodopsin induced a significant conformational change in the protein. Therefore, the phosphorylated carboxyl terminal end of rhodopsin seems to be directly involved in shaping the cytoplasmic surface of the photoreceptor protein into a conformation that is most likely associated with deactivation and termination of its signaling state.

Conflicts of interest

The authors declare that there is no conflict of interests regarding the publication of this article.

Authors' contributions

S. R., M.-L. S., G. B. and J. B. performed research and analyzed data. J.B. designed research and wrote the paper. All authors read and approved the final manuscript.

Acknowledgments

We want to thank Nelson A. Araujo and Deisy Perdomo for their assistance and valuable suggestions.

References

[1] K. Palczewski, G protein-coupled receptor rhodopsin, Annu. Rev. Biochem. 75 (2006) 743–767, https://doi.org/10.1146/annurev.biochem.75.103004.142743.
[2] Y.A. Ovchinnikov, Rhodopsin and bacteriorhodopsin: structure-function relationships, FEBS Lett. 148 (1982) 179–191, https://doi.org/10.1016/0014-5793(82)80805-3.

[3] P.A. Hargrave, J.H. McDowell, D.R. Curtis, J.K. Wang, E. Juszczak, S.L. Fong, J.K. Rao, P. Argos, The structure of bovine rhodopsin, Biophys. Struct. Mech. 9 (1983) 235–244, https://doi.org/10.1007/BF00535659.
[4] S.S. Karnik, T.P. Sakmar, H.B. Chen, H.G. Khorana, Cysteine residues 110 and 187 are essential for the formation of correct structure in bovine rhodopsin, Proc. Natl. Acad. Sci. U. S. A. 85 (1988) 8459–8463, https://doi.org/10.1073/pnas.85.22.8459.
[5] S.S. Karnik, H.G. Khorana, Assembly of functional rhodopsin requires a disulfide bond between cysteine residues 110 and 187, J. Biol. Chem. 265 (1990) 17520–17524.
[6] Y.A. Ovchinnikov, N.G. Abdulaev, A.S. Bogachuk, Two adjacent cysteine residues in the C-terminal cytoplasmic fragment of bovine rhodopsin are palmitylated, FEBS Lett. 230 (1988) 1–5, https://doi.org/10.1016/0014-5793(88)80628-8.
[7] D.I. Papac, K.R. Thornburgh, E.E. Büllesbach, R.K. Crouch, D.R. Knapp, Palmitylation of a G-protein coupled receptor. Direct analysis by tandem mass spectrometry, J. Biol. Chem. 267 (1992) 16889–16894.
[8] Y. Imamoto, M. Kataoka, F. Tokunaga, K. Palczewski, Light-induced conformational changes of rhodopsin probed by fluorescent alexa594 immobilized on the cytoplasmic surface, Biochemistry 39 (2000) 15225–15233, https://doi.org/10.1021/bi0018685.
[9] T. Mielke, U. Alexiev, M. Gläsel, H. Otto, M.P. Heyn, Light-induced changes in the structure and accessibility of the cytoplasmic loops of rhodopsin in the activated MII state, Biochemistry 41 (2002) 7875–7884, https://doi.org/10.1021/bi011862v.
[10] K. Yang, D.L. Farrens, C. Altenbach, Z.T. Farahbakhsh, W.L. Hubbell, H.G. Khorana, Structure and function in rhodopsin. Cysteines 65 and 316 are in proximity in a rhodopsin mutant as indicated by disulfide formation and interactions between attached spin labels, Biochemistry 35 (1996) 14040–14046, https://doi.org/10.1021/bi962113u.
[11] K. Cai, J. Klein-Seetharaman, J. Hwa, W.L. Hubbell, H.G. Khorana, Structure and function in rhodopsin: effects of disulfide cross-links in the cytoplasmic face of rhodopsin on transducin activation and phosphorylation by rhodopsin kinase, Biochemistry 38 (1999) 12893–12898, https://doi.org/10.1021/bi9912443.
[12] H. Yu, M. Kono, D.D. Oprian, State-dependent disulfide cross-linking in rhodopsin, Biochemistry 38 (1999) 12028–12032, https://doi.org/10.1021/bi990948+.
[13] A. Gelasco, R.K. Crouch, D.R. Knapp, Intrahelical arrangement in the integral membrane protein rhodopsin investigated by site-specific chemical cleavage and mass spectrometry, Biochemistry 39 (2000) 4907–4914, https://doi.org/10.1021/bi992736i.
[14] U. Wilden, H. Kühn, Light-dependent phosphorylation of rhodopsin: number of phosphorylation sites, Biochemistry 21 (1982) 3014–3022, https://doi.org/10.1021/bi00541a032.
[15] H. Ohguro, J.P. Van Hooser, A.H. Milam, K. Palczewski, Rhodopsin phosphorylation and dephosphorylation in vivo, J. Biol. Chem. 270 (1995) 14259–14262, https://doi.org/10.1074/jbc.270.24.14259.
[16] H. Ohguro, M. Rudnicka-Nawrot, J. Buczyłko, X. Zhao, J.A. Taylor, K.A. Walsh, K. Palczewski, Structural and enzymatic aspects of rhodopsin phosphorylation, J. Biol. Chem. 271 (1996) 5215–5224.
[17] A. Mendez, M.E. Burns, A. Roca, J. Lem, L.W. Wu, M.I. Simon, D.A. Baylor, J. Chen, Rapid and reproducible deactivation of rhodopsin requires multiple phosphorylation sites, Neuron 28 (2000) 153–164, https://doi.org/10.1016/S0896-6273(00)00093-3.
[18] T. Maeda, Y. Imanishi, K. Palczewski, Rhodopsin phosphorylation: 30 years later, Prog. Retin. Eye Res. 22 (2003) 417–434, https://doi.org/10.1016/S1350-9462(03)00017-X.
[19] A.W. Azevedo, T. Doan, H. Moaven, I. Sokal, F. Baameur, S.A. Vishnivetskiy, K.T. Homan, J.J. Tesmer, V.V. Gurevich, J. Chen, F. Rieke, C-terminal threonines and serines play distinct roles in the desensitization of rhodopsin, a G protein-coupled receptor, Elife 4 (2015), e05981, https://doi.org/10.7554/eLife.05981.
[20] N.S. Kosower, E.M. Kosower, G.L. Newton, H.M. Ranney, Bimane fluorescent labels: labeling of normal human red cells under physiological conditions, Proc. Natl. Acad. Sci. U. S. A. 76 (1979) 3382–3386, https://doi.org/10.1073/pnas.76.7.3382.
[21] M.V. Trivedi, J.S. Laurence, T.J. Siahaan, The role of thiols and disulfides on protein stability, Curr. Protein Pept. Sci. 10 (2009) 614–625, https://doi.org/10.2174/138920309789630534.
[22] J. Bubis, R. Medina, C. Möller, D. Perdomo, S. Rodríguez, N. Araujo, C. Sanz, I. Bello, Aproximaciones químicas para el estudio de la rodopsina, in: J. Wilkesman, L. Kurz (Eds.), Memorias del Colloquium Biochimie: Bioquímica y sus aplicaciones, Cuvillier Verlag, Göttingen, 2016, pp. 60–96.
[23] J. Bubis, Effect of detergents and lipids on transducin photoactivation by rhodopsin, Biol. Res. 31 (1998) 59–71.
[24] W. Godchaux III, W.F. Zimmerman, Soluble proteins of intact bovine rod cell outer segments, Exp. Eye Res. 28 (1979) 483–500, https://doi.org/10.1016/0014-4835(79)90123-4.
[25] H. Kühn, Light- and GTP-regulated interaction of GTPase and other proteins with bovine photoreceptor membranes, Nature 283 (1980) 587–589, https://doi.org/10.1038/283587a0.
[26] G. Wald, P.K. Brown, The molar extinction of rhodopsin, J. Gen. Physiol. 37 (1953) 189–200, https://doi.org/10.1085/jgp.37.2.189.
[27] R. Medina, D. Perdomo, J. Bubis, The hydrodynamic properties of dark- and light-activated states of n-dodecyl β-D-maltoside-solubilized bovine rhodopsin support the dimeric structure of both conformations, J. Biol. Chem. 279 (2004) 39565–39573, https://doi.org/10.1074/jbc.M402446200.
[28] U.K. Laemmli, Cleavage of structural proteins during the assembly of the head of bacteriophage T4, Nature 227 (1970) 680–685, https://doi.org/10.1038/227680a0.
[29] J. Klein-Seetharaman, E.V. Getmanova, M.C. Loewen, P.J. Reeves, H.G. Khorana, NMR spectroscopy in studies of light-induced structural changes in mammalian rhodopsin: applicability of solution ^{19}F NMR, Proc. Natl. Acad. Sci. U. S. A. 96 (1999) 13744–13749, https://doi.org/10.1073/pnas.96.24.13744.
[30] D.L. Farrens, C. Altenbach, K. Yang, W.L. Hubbell, H.G. Khorana, Requirement of rigid-body motion of transmembrane helices for light activation of rhodopsin, Science 274 (1996) 768–770, https://doi.org/10.1126/science.274.5288.768.
[31] D.J. Pappin, J.B. Findlay, Sequence variability in the retinal-attachment domain of mammalian rhodopsins, Biochem. J. 217 (1984) 605–613, https://doi.org/10.1042/bj2170605.
[32] M.M. Bradford, A rapid and sensitive method for the quantitation of microgram quantities of protein utilizing the principle of protein-dye binding, Anal. Biochem. 72 (1976) 248–254, https://doi.org/10.1016/0003-2697(76)90527-3.
[33] H. Towbin, T. Staehelin, J. Gordon, Electrophoretic transfer of proteins from polyacrylamide gels to nitrocellulose sheets: procedure and some applications, Proc. Natl. Acad. Sci. U. S. A. 76 (1979) 4350–4354, https://doi.org/10.1073/pnas.76.9.4350.
[34] B. Tasheva, G. Dessev, Artifacts in sodium dodecyl sulfate-polyacrylamide gel electrophoresis due to 2-mercaptoethanol, Anal. Biochem. 129 (1983) 98–102, https://doi.org/10.1016/0003-2697(83)90057-X.
[35] U. Alexiev, D.L. Farrens, Fluorescence spectroscopy of rhodopsins: insights and approaches, Biochim. Biophys. Acta Bioenerg. 1837 (2014) 694–709, https://doi.org/10.1016/j.bbabio.2013.10.008.
[36] H.W. Choe, Y.J. Kim, J.H. Park, T. Morizumi, E.F. Pai, N. Krauss, K.P. Hofmann, P. Scheerer, O.P. Ernst, Crystal structure of metarhodopsin II, Nature 471 (2011) 651–655, https://doi.org/10.1038/nature09789.
[37] T.D. Dunham, D.L. Farrens, Conformational changes in rhodopsin. Movement of helix F detected by site-specific chemical labeling and fluorescence spectroscopy, J. Biol. Chem. 274 (1999) 1683–1690, https://doi.org/10.1074/jbc.274.3.1683.
[38] J.G. Krupnick, V.V. Gurevich, J.L. Benovic, Mechanism of quenching of phototransduction. Binding competition between arrestin and transducin for phosphorhodopsin, J. Biol. Chem. 272 (1997) 18125–18131, https://doi.org/10.1074/jbc.272.29.18125.
[40] K. Kirchberg, T.Y. Kim, M. Möller, D. Skegro, G. Dasara Raju, J. Granzin, G. Büldt, R. Schlesinger, U. Alexiev, Conformational dynamics of helix 8 in the GPCR rhodopsin controls arrestin activation in the desensitization process, Proc. Natl. Acad. Sci. U. S. A. 108 (2011) 18690–18695, https://doi.org/10.1073/pnas.1015461108.
[41] W.T. Mason, R.S. Fager, E.W. Abrahamson, Lipid and fatty acid composition of frog photoreceptor outer segments, Biochemistry 12 (1973) 2147–2150, https://doi.org/10.1021/bi00735a021.
[42] A.D. Albert, J.E. Young, Z. Paw, Phospholipid fatty acyl spatial distribution in bovine rod outer segment disk membranes, Biochim. Biophys. Acta Biomembr. 1368 (1988) 52–60, https://doi.org/10.1016/S0005-2736(97)00200-9.
[43] D.C. Mitchell, M. Straume, B.J. Litman, Role of *sn*-1-saturated,*sn*-2-polyunsaturated phospholipids in control of membrane receptor conformational equilibrium: effects of cholesterol and acyl chain unsaturation on the metarhodopsin I ↔ metarhodopsin II equilibrium, Biochemistry 31 (1992) 662–670, https://doi.org/10.1021/bi00118a005.
[44] D.C. Mitchell, J.T. Lawrence, B.J. Litman, Primary alcohols modulate the activation of the G protein-coupled receptor rhodopsin by a lipid-mediated mechanism, J. Biol. Chem. 271 (1996) 19033–19036, https://doi.org/10.1074/jbc.271.32.19033.
[45] D.C. Mitchell, S.L. Niu, B.J. Litman, DHA-rich phospholipids optimize G-Protein-coupled signaling, J. Pediatr. 143 (Supplement) (2003) 80–86, https://doi.org/10.1067/S0022-3476(03)00405-0.
[46] W.E. Teague Jr., O. Soubias, H. Petrache, N. Fuller, K.G. Hines, R.P. Rand, K. Gawrisch, Elastic properties of polyunsaturated phosphatidylethanolamines influence rhodopsin function, Faraday Discuss 161 (2013) 383–395, https://doi.org/10.1039/C2FD20095C.
[47] M.P. Bennett, D.C. Mitchell, Regulation of membrane proteins by dietary lipids: effects of cholesterol and docosahexaenoic acid acyl chain-containing phospholipids on rhodopsin stability and function, Biophys. J. 95 (2008) 1206–1216, https://doi.org/10.1529/biophysj.107.122788.
[48] O. Soubias, K. Gawrisch, The role of the lipid matrix for structure and function of the GPCR rhodopsin, Biochim. Biophys. Acta Biomembr. 1818 (2012) 234–240, https://doi.org/10.1016/j.bbamem.2011.08.034.
[49] L.A. Salas-Estrada, N. Leioatts, T.D. Romo, A. Grossfield, Lipids alter rhodopsin function via ligand-like and solvent-like interactions, Biophys. J. 114 (2018) 355–367, https://doi.org/10.1016/j.bpj.2017.11.021.
[50] S.E. Mansoor, H.S. McHaourab, D.L. Farrens, Mapping proximity within proteins using fluorescence spectroscopy. A study of T4 lysozyme showing that tryptophan residues quench bimane fluorescence, Biochemistry 41 (2002) 2475–2484, https://doi.org/10.1021/bi011198i.
[51] L.D. Islas, W.N. Zagotta, Short-range molecular rearrangements in ion channels detected by tryptophan quenching of bimane fluorescence, J. Gen.

Physiol. 128 (2006) 337–346, https://doi.org/10.1085/jgp.200609556.
[52] A.M. Jones Brunette, D.L. Farrens, Distance mapping in proteins using fluorescence spectroscopy: tyrosine, like tryptophan, quenches bimane fluorescence in a distance-dependent manner, Biochemistry 53 (2014) 6290–6301, https://doi.org/10.1021/bi500493r.
[53] M. Dorey, P.A. Hargrave, J.H. McDowell, A. Arendt, T. Vogt, N. Bhawsar, A.D. Albert, P.L. Yeagle, Biochim. Biophys. Acta Biomembr. 1416 (1999) 217–224, https://doi.org/10.1016/S0005-2736(98)00224-7.
[54] O.G. Kisselev, J.H. McDowell, P.A. Hargrave, The arrestin-bound conformation and dynamics of the phosphorylated carboxy-terminal region of rhodopsin, FEBS Lett. 564 (2004) 307–311, https://doi.org/10.1016/S0014-5793(04)00226-1.
[55] E. Getmanova, A.B. Patel, J. Klein-Seetharaman, M.C. Loewen, P.J. Reeves, N. Friedman, M. Sheves, S.O. Smith, H.G. Khorana, NMR spectroscopy of phosphorylated wild-type rhodopsin: mobility of the phosphorylated C-terminus of rhodopsin in the dark and upon light activation, Biochemistry 43 (2004) 1126–1133, https://doi.org/10.1021/bi030120u.
[56] O.G. Kisselev, M.A. Downs, J.H. McDowell, P.A. Hargrave, Conformational changes in the phosphorylated C-terminal domain of rhodopsin during rhodopsin arrestin interactions, J. Biol. Chem. 279 (2004) 51203–51207, https://doi.org/10.1074/jbc.M407341200.
[57] Y. Kang, X.E. Zhou, X. Gao, Y. He, W. Liu, A. Ishchenko, A. Barty, T.A. White, O. Yefanov, G.W. Han, Q. Xu, P.W. de Waal, J. Ke, M.H. Tan, C. Zhang, A. Moeller, G.M. West, B.D. Pascal, N. Van Eps, L.N. Caro, S.A. Vishnivetskiy, R.J. Lee, K.M. Suino-Powell, X. Gu, K. Pal, J. Ma, X. Zhi, S. Boutet, G.J. Williams, M. Messerschmidt, C. Gati, N.A. Zatsepin, D. Wang, D. James, S. Basu, S. Roy-Chowdhury, C.E. Conrad, J. Coe, H. Liu, S. Lisova, C. Kupitz, I. Grotjohann, R. Fromme, Y. Jiang, M. Tan, H. Yang, J. Li, M. Wang, Z. Zheng, D. Li, N. Howe, Y. Zhao, J. Standfuss, K. Diederichs, Y. Dong, C.S. Potter, B. Carragher, M. Caffrey, H. Jiang, H.N. Chapman, J.C. Spence, P. Fromme, U. Weierstall, O.P. Ernst, V. Katritch, V.V. Gurevich, P.R. Griffin, W.L. Hubbell, R.C. Stevens, V. Cherezov, K. Melcher, H.E. Xu, Crystal structure of rhodopsin bound to arrestin by femtosecond X-ray laser, Nature 523 (2015) 561–567, https://doi.org/10.1038/nature14656.
[58] X.E. Zhou, K. Melcher, H.E. Xu, Understanding the GPCR biased signaling through G protein and arrestin complex structures, Curr. Opin. Struct. Biol. 45 (2017) 150–159, https://doi.org/10.1016/j.sbi.2017.05.004.
[59] X.E. Zhou, Y. He, P.W. de Waal, X. Gao, Y. Kang, N. Van Eps, Y. Yin, K. Pal, D. Goswami, T.A. White, A. Barty, N.R. Latorraca, H.N. Chapman, W.L. Hubbell, R.O. Dror, R.C. Stevens, V. Cherezov, V.V. Gurevich, P.R. Griffin, O.P. Ernst, K. Melcher, H.E. Xu, Identification of phosphorylation codes for arrestin recruitment by G protein-coupled receptors, Cell 170 (2017) 457–469, https://doi.org/10.1016/j.cell.2017.07.002.